Effect of *ex-situ* post-annealing treatments on Sr_2FeMoO_6 thin films

M. Metsänoja · S. Majumdar · H. Huhtinen · P. Paturi

Abstract Magnetoresistive Sr_2FeMoO_6 thin films were grown by pulsed laser deposition at optimized deposition atmosphere and temperature. Films were then *ex-situ* post-annealed in different atmospheres and by vacuum annealing at temperatures between 500°C and 1100°C. Ar and air annealed samples were destroyed by *ex-situ* post-annealing treatment, due to formation and dominance of $SrMoO_4$ impurity phase. X-ray diffraction showed no impurities and full texturation of vacuum and $ArH_2(5\%)$ annealed samples. Those samples showed also similar magnetic and magnetoresistive behaviour like as-deposited sample. Neither magnetic, magnetotransport nor structural properties could be improved by *ex-situ* post-annealling treatments.

Keywords Strontium iron molybdate · Thin films · Double perovskite · Pulsed laser deposition

1 Introduction

The double perovskite Sr_2FeMoO_6 (SFMO) has been widely studied after the discovery of its high Curie temperature, T_C around 410–450 K [1–4] and exceptionally large intrinsic tunnel magnetoresistance at room temperature [1]. As a half-metallic material SFMO has high spin polarization (up to 0.75 estimated by point-contact spectroscopy [5]) at room temperature [6,7]. Therefore SFMO has great potential for spintronic and magnetoresistive applications. The applications require high quality thin films with smooth surface and T_C clearly above room temperature to achieve as high spin polarization as possible. Fabricating good quality SFMO

M. Metsänoja · S. Majumdar · H. Huhtinen · P. Paturi
Wihuri Physical Laboratory, Department of Physics and Astronomy, University of Turku, FI-20014 Turku, Finland
E-mail: minnamari.metsanoja@utu.fi tel. +358-2-333 5942

thin films has nevertheless proven to be difficult [8,9] because of fairly extreme preparation conditions such as high growth temperature and relatively high vacuum.

Pulsed laser deposition (PLD) appears to be the best method to reach high quality SFMO thin films [8, 10,11], even though there are several other fabrication methods like chemical vapor process [3]. Advantages of PLD are that it does not require very a high vacuum during the deposition and a stoichiometric target can be used [9,10]. Commonly used atmosphere in the deposition of SFMO thin films is oxygen [10,12–14], but vacuum, Ar, N_2, or mixture of these with O_2 and H_2 are also used [13–15]. The choice of the deposition atmosphere has a crucial role in the deposition process as well as the deposition temperature. It has been shown that the oxygen background pressure higher than 10^{-4} mbar leads to formation of impurity phases, normally $SrMoO_4$ [12,16]. Other typical impurity in polycrystalline and thin film SFMO samples is Fe, but impurities like Fe_3O_4, $SrFeO_3$ and $SrMoO_3$ are also possible [8,17]. SFMO thin films with no indication of different phases, orientations or impurities have been made with $Ar/H_2(5\ \%)$ deposition atmosphere and at deposition temperature of 1050°C [8,11]. It has been also shown that by varying the $Ar/H_2(5\ \%)$ background pressure between 0.005 Torr and 0.1 Torr, notable changes in the magnetic properties of the thin films are not observed [11].

Usually polycrystalline samples have T_C close to the theoretical and literature value of 450 K, but thin films with that high T_C have not yet made. Highest onset T_C values of the thin films prepared in optimized deposition atmosphere and temperature were about 375 K, even though T_C of the target used in deposition of these films was around 400 K [11]. With other deposition atmospheres T_C over room temperature have been achieved,

but not proven values close to 400 K [12–15]. One of the possible reasons for changes in the magnetic properties between the polycrystalline and the thin film samples growth by PLD can be the anti-site disorder (ASD) in which Fe and Mo transpose. The fabrication process of polycrystalline sample is long compared to the deposition of the thin films. Sintering time of the SFMO target is around 12 h [11], when the deposition time of the films is around 10 minutes. Longer time gives the material more time to settle and it has been shown that low growth rate and therefore longer growth time results better cationic ordering in SFMO[18]. Properties of thin films have also been improved by adding small amounts of oxygen after the deposition, which could indicate that the oxygen vacancies are the cause of lower T_C values. ASD level has been proved to affect the magnetisation, T_C and spin polarization of SFMO [19,20] and it is shown that ASD decreases in polycrystalline samples with increasing sintering temperature up to 1200°C [21]. Post-annealing treatments of manganite thin films, which have similar ferromagnetic (FM) and half-metallic properties like SFMO, show significant
modification in their structural and magnetic properties [22,23]. So it is expected that post-annealing treatments will affect also the properties of the SFMO thin films.

In this paper we have fabricated SFMO thin films with optimized deposition atmosphere and temperature and investigated the effects of *ex-situ* post-annealing treatments on the magnetic properties of the thin films. Post-annealing treatments were carried out in Ar, Ar/H$_2$(5 %) and air atmosphere and by vacuum annealing at different temperatures between 500°C and 1100°C.

2 Experimental details

Thin films of SFMO were deposited on SrTiO$_3$ single crystal substrates by pulsed laser deposition at deposition temperature of 1050°C and Ar/H$_2$(5 %) atmosphere at 11 Pa pressure. Details of the film deposition are reported in [11]. Stoichiometric target used in deposition was prepared from nanograined powder fabricated by the sol-gel method. Powder preparation is described in [24,25] and sample preparation from powder to target is described in detail in [11].

Ex-situ post-annealing treatments were carried out to four as-deposited SFMO thin films. Before treatments all as-deposited films were cut into four pieces. Treatments were done in Ar, Ar/H$_2$(5 %) and air atmosphere and by vacuum annealing. Post-annealing temperatures were 500°C, 700°C, 900°C and 1100°C. Sam-

ples were heated to the desired temperature in five hours and kept there for 10 hours. Samples were cooled down to room temperature in 8 (500°C), 12 (700°C), 15 (900°C) and 18 (1100°C) hours.

X-ray diffraction (XRD) was used to determine structural properties of the films. Measurements were made with Philips X'pert Pro MPD diffractometer with a Schultz texture goniometer before and after post-annealing treatments to ensure uniform quality and to enable comparison of the results. Phase purity and orientation were determined from the $2\theta-\theta$-scans. Texture measurements were carried out for the SFMO (204) peaks at $2\theta = 57.16°$, because it does not overlap with the substrate peak, and for typical impurity peaks of Fe (110) at $2\theta = 44.98°$ and SrMoO$_4$ (112) at $2\theta = 27.68°$. SFMO (204) peak was measured in more detail with $2\theta - \phi$ scan to determine lattice parameters and strain of the films. Surface structure and root mean square (RMS) roughness of the films were defined from atomic force microscopy (AFM) images.

Magnetic properties of the films were determined with a Cryogenic SQUID magnetometer. Zero-field cooled (ZFC) and field-cooled (FC) curves were measured in 0.1 T. Temperature and magnetic field dependence of resistivity were also measured for as-deposited and one vacuum annealed film with a Quantum Design Physical Property Measurement System (PPMS).

3 Results and discussion

3.1 Structural properties

According to the XRD measurements, all as-deposited films have uniform quality and they are similar as reported in [11]. The 2θ-scans of vacuum and ArH$_2$(5 %) annealed films showed only SFMO (00l) peaks and the SFMO pole figures revealed predictably clear sharp (204) and (132) peaks like results for as-deposited films. No texture were observed in Fe and SrMoO$_4$ impurity phase peaks. Both 2θ-scans and texture measurements indicate no impurities in vacuum and ArH$_2$(5 %) annealed samples by the XRD in the detection limit of around 1%. In 2θ-scan of Ar annealed sample only the peaks of the substrate were clearly detected. The pole figures of Ar annealed film are shown in Fig. 1. There are no clear SFMO peaks visible, as can be seen from Fig. 1a. Instead SrMoO$_4$ pole figures (Fig. 1c) have clear peaks indicating the presence of SrMoO$_4$ impurity phase. In these samples the Fe impurity (Fig. 1b) was not detected. Also the yellowish brown color of the Ar annealed sample indicates that most of the sample is SrMoO$_4$ [24]. All the air annealed samples had also bright yellow color indicating that the majority phase
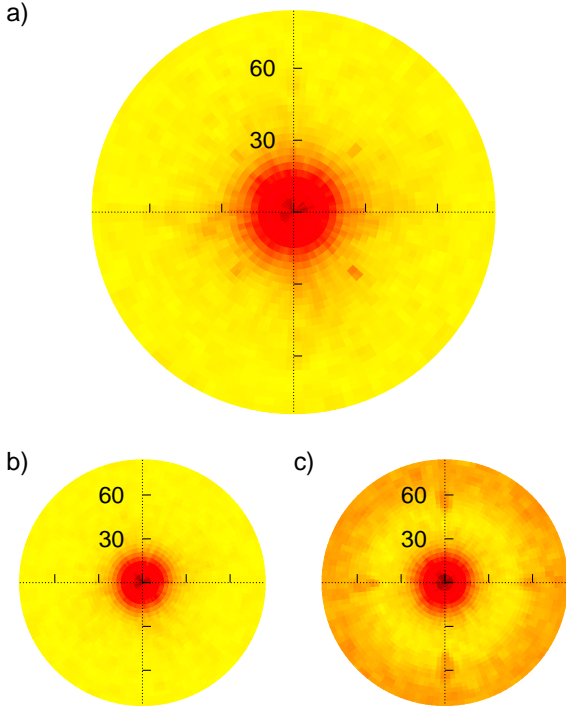
Fig. 1 Pole figures in the logarithmic scale of the a) SFMO (204) and (132) peaks, b) Fe (110) and c) $SrMoO_4$ (112) peaks for film Ar annealed at 900 °C.

Fig. 2 The ZFC and FC magnetization curves at 0.1 T for as deposited film and films post-annealed at 900°C. Note that vacuum annealed is shown on the right hand scale.

is $SrMoO_4$ instead of SFMO. From that we concluded that air annealed samples were destroyed as a result of the post-annealing and no further measurements were carried out to those samples.

The lattice parameters of vacuum and ArH_2(5 %) annealed films were obtained from $\theta-2\theta$ scan and $2\theta-\phi$ scan of SFMO (204) peak. For Ar annealed film the SFMO (204) peak was not observed. ArH_2(5 %) annealing did not affect lattice parameter c, but $a = b$ decreased from as-deposed value 5.82 Å to 5.76 Å. Vacuum annealing increased the lattice parameter c from 7.79 Å to 7.85 Å and $a = b$ from 5.82 Å to 5.91 Å. The 2θ full width at half maximum (FWHM) of (204) peak of the ArH_2(5 %) annealed film narrowed 19.5 % (0.12°). Corresponding value for vacuum annealed film narrowed 3.8 % (0.02°). ϕ FWHM narrowed 5.4 % (0.03°) for ArH_2(5 %) annealed and 18.0 % (0.09°) for vacuum annealed film. These suggest that *ex-situ* post-annealing treatments slightly change the volume of unit cell and for ArH_2(5 %) annealed sample decrease the mismatch between the film and substrate. The cause of these changes is most likely the removal of oxygen from the film resulting in an increased bond length.

RMS-roughnesses of the films were determined from the AFM images. For all as-deposited films RMS rough-
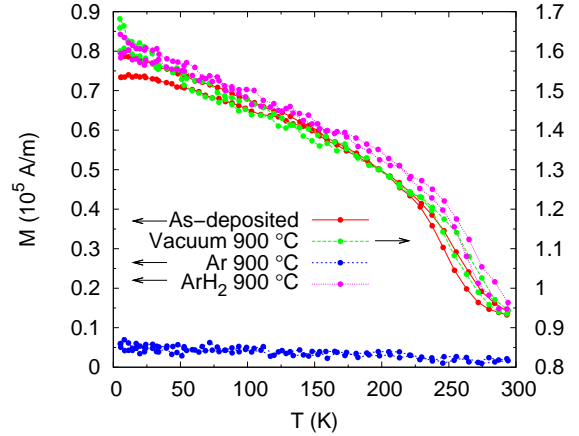
ness values vary between 2.7 nm and 4.5 nm as measured from the averages of 2x2 μm^2, 5x5 μm^2, 10x10 μm^2 and 20x20 μm^2 scans. Because the variation in RMS values is minor, we can assume that as-deposited films had uniform quality. For vacuum and ArH_2(5%) annealed films, which are pure SFMO in the XRD detection limit, RMS roughness values are similar like as-deposited films. A clear increase in roughness values with the annealing temperature was observed in Ar annealed films. Values increased from the 5.372 nm (annealed at 500 °C) to 39.07 nm (annealed at 1100 °C). The major change in the RMS roughness values between Ar and ArH_2(5%) or vacuum annealed film could be related to the fact that most of the Ar annealed sample is $SrMoO_4$.

3.2 Magnetic properties

The ZFC and FC magnetization as a function of temperature is shown in Fig. 2 for films as-deposited and post-annealed at 900°C. Vacuum and ArH_2(5 %) annealing did not improve nor worsen magnetic properties of the films. Both films have FM-PM transition at the same temperature as as-deposited film and the shapes of the transitions are identical. These samples has also paramagnetic moment above T_C which is for ArH_2(5 %) annealed sample as high as in as-deposited sample and for vacuum annealed sample rather larger. The paramagnetic moment above T_C can been explained by additional ferromagnetic impurity phase which is undetectable by XRD. 1% of metallic Fe would cause a magnetic signal around $0.18 \cdot 10^5$ A/m which is as large as detected for as-deposited and ArH_2(5 %) annealed samples and it is under the XRD detection limit. Metallic Fe can not however explain the magnetic moment of
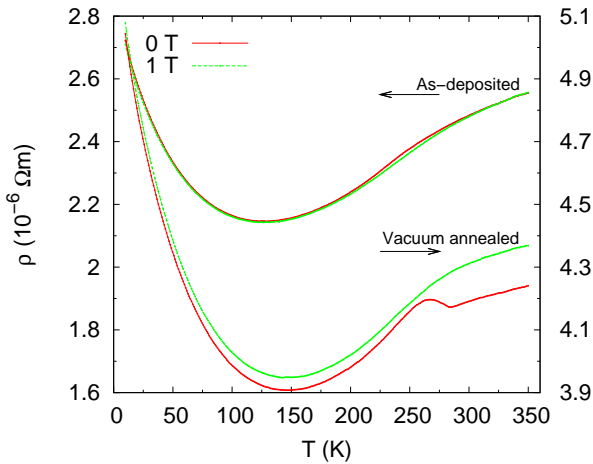
Fig. 3 Resistivity as a function of temperature in 0 T and 1 T fields for as-deposited film (left scale) and film vacuum annealed at 700°C (right scale.

Fig. 4 Field dependences of the magnetoresitivity for as-deposited film at different temperatures between 10 K and 350 K.

Fig. 5 Field dependences of the magnetoresitivity at different temperatures between 10 K and 350 K for film vacuum annealed at 700°C.

the vacuum annealed sample Fig. 2 above SFMO T_C because that large magnetic signal would require 5% of Fe, which would have been detected with XRD. Typical impurity $SrMoO_4$ is non-magnetic and $SrMoO_3$ is so weakly magnetic that they could not cause the effect. Neither the possible impurity $SrFeO_3$ as a antiferromagnetic material can not be the reason for the magnetic signal. So there is a possibility that Fe_3O_4 or some other magnetic impurity undetectable by XRD is present. Also metallic Fe could be present in a form undetectable by XRD like noncrystallized nanoparticles. As seen from XRD measurements Ar annealed sample is mostly non-magnetic $SrMoO_4$ so magnetisation is practically zero at the whole temparature range from 5 K to 300 K. There was no significant changes in the magnetic properties of the films related to the annealing temperature.

3.3 Magnetoresistivity measurements

Temperature dependence of resistivity for as-deposited film and film vacuum annealed at 700°C are shown in Fig. 3. All the curves have a minimum around 130 K. For vacuum annealed film the resistivity is clearly increased from the as-deposited film on the whole temperature scale and the changes in resistivity with temperature are larger.

Magnetoresistance, $MR = (R_B - R_0)/R_0$, as a function of applied field at different temperatures for as deposited film is shown in Fig. 4 and for film vacuum annealed at 700°C in Fig. 5. For as-deposited film magnetoresistivity measurements show up to 6 % negative MR at 10 K and for vacuum annealed film slightly smaller. Similar MR values for SFMO thin films have
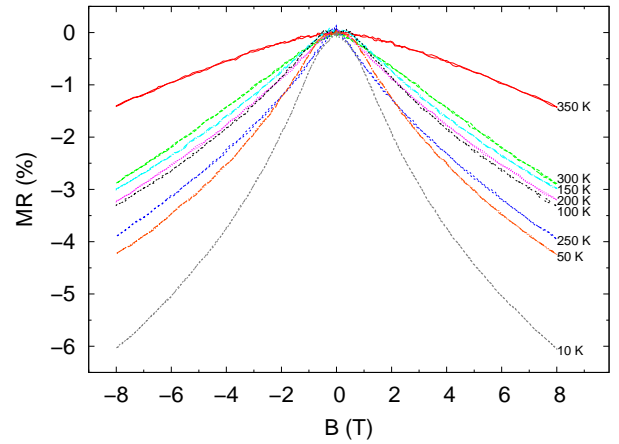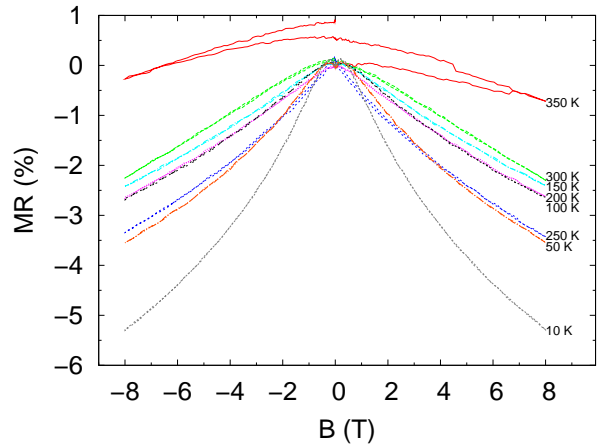
been reported in [10] and slightly larger values for polycrystalline sample in [26]. Results for as-deposited film shown no hysteretic behaviour at any temperatures and hysteresis is observed at 350 K for the vacuum annealed film as seen in Fig. 5. The slope of the curves increases when the measuring temperature decreases similarly as reported in [10]. Also the shape of curves changes when the measuring temperature rises from 300 K to 350 K (Figs. 4 and 5) indicating that FM-PM transition and therefore also the T_C of these samples are between 300 K and 350 K. Similar values for T_C can be determined also from the Fig. 2. Hence from the structural, magnetic and magnetotransport measurements it is shown that the *ex-situ* post-annealing treatments have no significant effect on the structural and magnetic properties of the SFMO films.

4 Conclusions

We have studied effects of *ex-situ* post-annealing treatments on SFMO thin films. Treatments were done in Ar, $ArH_2(5\%)$ and air atmospheres and by vacuum annealing at temperatures between $500°C$ and $1100°C$. Structural, magnetic and magnetotransport measurements did not show significant modification in the properties of the post-annealed films compared with as-deposited film. From that we conclude that *ex-situ* post-annealing treatments do not improve the T_C nor surface smoothness required for high quality films for spintronic applications. If the cause of lower T_C is the ASD or oxygen content, the improvement could be made with insitu post-annealing treatments or controlling the oxygen level during the deposition or treatments.

Acknowledgements

References

1. Kobayashi, K. I., Kimura, T., Sawada, H., Terakura, K., Tokura, Y.: Nature **395**, 677 (1998)
2. Sarma, D. D., Mahadevan, P., Saha-Dasgupta, T., Ray, S., Kumar, A.: Phys. Rev. Lett. **85**, 2549 (2000)
3. Rager, J., Berenov, A. V., Cohen, L. F., Branford, W. R., Bugoslavsky, Y. V., Miyoshi, Y., Ardakani, M., MacManus-Driscoll, J. L.: Appl. Phys. Lett. **81**, 5003 (2002)
4. Yuan, C. L., Zhu, Y., Ong, P. P., Ong, C. K., Yu, T., Shen, Z. X.: Physica B **334**, 408 (2003)
5. Bugoslavsky, Y., Miyoshi, Y., Clowes, S. K., Branford, W. R., Lake, M., Brown, I., Caplin, A. D., Cohen, L. F.: Phys. Rev. B **71**, 104523 (2005)
6. Tomioka, Y., Okuda, T., Okimoto, Y., Kumai, R., Kobayashi, K. I., Tokura, Y.: Phys. Rev. B **61**, 422 (2000)
7. Sarma, D., Sampathkumaran, E., Ray, S., Nagarajan, R., Majumdar, S., Kumar, A., Nalini, G., Row, T. G.: Solid State Communications **114**, 465 (2000)
8. Suominen, T., Raittila, J., Paturi, P.: Thin Solid Films **517**, 5793 (2009)
9. Kumar, D., Kaur, D.: Physica B **405**, 3259 (2010)
10. Manako, T., Izumi, M., Konishi, Y., Kobayashi, K. I., Kawasaki, M., Tokura, Y.: Appl. Phys. Lett. **74**, 2215 (1999)
11. Paturi, P., Metsänoja, M., Huhtinen, H.: Thin Solid Films **519**, 8047 (2011)
12. di Trolio, A., Larciprete, R., Testa, A. M., Fiorani, D., Imperatori, P., Turchini, S., Zema, N.: J. Appl. Phys. **100**, 013907 (2006)
13. Shinde, S. R., Ogale, S. B., Greene, R. L., Venkatesan, T., Tsoi, K., Cheong, S. W., Millis, A. J.: J. Appl. Phys. **93** 1605 (2003)
14. Venimadhav, A., Sher, F., Attfield, J. P., Blamire, M. G.: J. Magn. and Magn. Mater. **269** 101 (2004)
15. Borges, R. P., Lhostis, S., Bari, M. A., Versluijs, J. J., Lunney, J. G, Coey, J. M. D., Besse, M., Contour, J. P.: Thin Solid Films **429** 5 (2003)
16. Westerburg, W., Reisinger, D., Jakob, G.: Phys. Rev. B **62**, R767 (2000)
17. Santiso, J., Figueras, A., Fraxedas, J.: Surf. Interface Anal. **33**, 676 (2002)
18. Sánchez, D., García-Hernández, M., Auth, N., Jakob, G.: J. Appl. Phys. **96** 2736 (2004)
19. Park, B. J., Han, H., Kim, J., Kim, Y. J., Kim, C. S., Lee, B. W.: J. Magn. and Magn. Mater. **272-276**, 1851 (2004)
20. Aguilar, B., Navarro, O., Avignon, M.: Microelectronics Journal **39**, 560 (2008)
21. Balcells, L., Navarro, J., Bibes, M., Roig, A., Martinez, B., Fontcuberta, J.: Appl. Phys. Lett. **78**, 781 (2001)
22. Namikawa, T., Kaneta, K., Matsushita, N., Nakagawa, S., Naoe, M.: IEEE T. Magn. **35**, 2850 (1999)
23. Hsu, L. S., Liu, C. J., Wu, T. W., Luca, D.: Journal of Optoelectronics and Advanced Materials **5**, 409 (2003)
24. Raittila, J., Salminen, T., Suominen, T., Schlesier, K., Paturi, P.: J. Phys. Chem. Solids **67**, 1712 (2006)
25. Suominen, T., Raittila, J., Salminen, T., Schlesier, K., Linden, J., Paturi, P.: J. Magn. and Magn. Mater. **309**, 278 (2007)
26. Ray, S., Middey, S., Jana, S., Banerjee, A., Sanyal, P., Rawat, R., Gregoratti, L.: Europhys. Lett. **94**, 47007 (2011)